

Chapter 2

Study of highly sensitivity metal wires assisted photonic crystal fiber based refractive index sensor

In this chapter, a metal wire based photonic crystal fiber refractive index sensor has been designed and simulated using finite element method (FEM) based on COMSOL Multiphysics software. We have compared among three plasmonic materials copper, gold, and silver based PCF sensor on the basis of wavelength sensitivity, amplitude sensitivity, resolution, and figure of merit parameters for the analyte sample range of RI $n_a = 1.31 - 1.36$. Among them copper based PCF sensor structure is highly sensitive with high figure of merit. Hence this copper metal wire based PCF sensor is cost – efficient for different sensing application in different fields.

2.1 Introduction

A new technology based on surface plasmon resonance (SPR) has achieved rapid development in the last decades. Recently, SPR based optical fiber sensor has been attracted to detect gases like Cl, H₂, and N₂ and also some toxic gases like NH₃, H₂S⁸⁵. It has also been used to analyze the quality of food, its composition, and the concentration of components⁸⁶, biological materials, and toxic metals detection⁸⁷. In 1968, Andreas Otto devised a prism coupling setup based on attenuated total reflection (ATR) that enables the coupling of surface plasmon waves with the evanescent wave⁶⁵. Kretschman modified such a device with a coated metal layer on the prism base. A metal layer is in direct contact with the dielectric medium of the smaller refractive index⁸⁸. A p-polarized light incident on the prism-metal interface through the prism at an angle greater or equal to θ_{ATR} , the evanescent wave is propagated at the interface. Excitation of surface plasmon takes place at the same frequency for that propagation constant of the evanescent wave corresponds with that of surface plasmon. This method is suitable for SPR sensing, but it is bulky in size and costly⁸⁹. So it has many limitations in practical applications. On the other side, photonic crystal fiber solves all these issues due to its small size with low loss. Compare to other optical fibers, PCF is flexible in design, and its geometry can be altered by changing the radius of air holes to manage the light propagation to gain better sensitivity and less confinement loss⁹⁰. Two kinds of PCF structures are generally used for SPR sensing. In the first kind of PCF structure, the layer of metal is coated inside the air holes^{91 73}. Such a PCF design was presented by⁷⁴ and reported the sensitivity of 2000 nm/RIU. Such sensors lifted the sensitivity with better detection abilities, but it has low mobility and slow detection speed^{92 93}.

Chapter 2: Metal wires assisted PCF based refractive index sensor

In the other kind of PCF structure, a metal layer is coated at the outer side of the fiber, and at the time of measurement whole sensor is in contact with the sensing medium^{94 95}. Recently, reported papers^{95 96 97} have worked on such a sensor using gold as a plasmonic material to obtain maximum wavelength sensitivity 2200 nm/ RIU, 4200 nm/RIU, 5000 nm/RIU with sensor resolution of 3.75×10^{-5} RIU, 2.4×10^{-5} RIU, 2.0×10^{-5} RIU, respectively. In their presented PCF designs, a coating of thin gold layer has been used to generate the surface plasmons. This method simplifies the structure of manufacturing and implementation, but the uneven thickness of the metal layer is still a problem that cannot be ignored.

In this study, we have presented a design of a highly sensitive metal wire-assisted solid-core PCF sensor using different metal wires like Cu, Au, and Ag. Metal wires solve the issues of uneven thickness of the metal coating, enhance resonance effect as well as improve the sensitivity of the proposed sensor^{98 99}. The fabrication of the proposed PCF structure is easy and flexible. Circular holes pattern of PCF is fabricated by using conventional stack-and-draw technique¹⁰⁰ in which macroscopic elements of the fiber is prepared by stacking glass rod according to the required design and then it is drawn into microstructure rods. This process continues until researchers get the desired structure. Other methods, such as capillary stacking and the die-cast process may also be used for fabrication¹⁰¹. Metal wire can directly be attached to the cladding surface. Numerical simulation is performed by the finite element method (FEM) based on COMSOL Multiphysics software. We have investigated the confinement loss, sensitivity, and resolution of the proposed PCF sensor for different structure parameters such as air holes radius, metal wire radius for the considered metals. A comparative study and discussion have also presented among chosen metals. Finally, we have concluded our results.

Chapter 2: Metal wires assisted PCF based refractive index sensor

2.2 Model and theoretical analysis

The structure of metals wire assisted solid-core PCF is depicted in figure 2.1. In order to achieve better sensitivity, we have used inner holes in the form of hexagonal that generates a higher evanescent field than circular shapes when they have the same air filling fraction¹⁰². The proposed sensor has a solid core with the inner hole around the core of radius r_a arranged in the form of a hexagon. There are two outer layers of holes with radius r_b , and r_c surround the core. One diametric line is missing which provides a convenient path to propagate the light on to the metal surface. In the outer layer, there is an analyte channel with two metal wires.

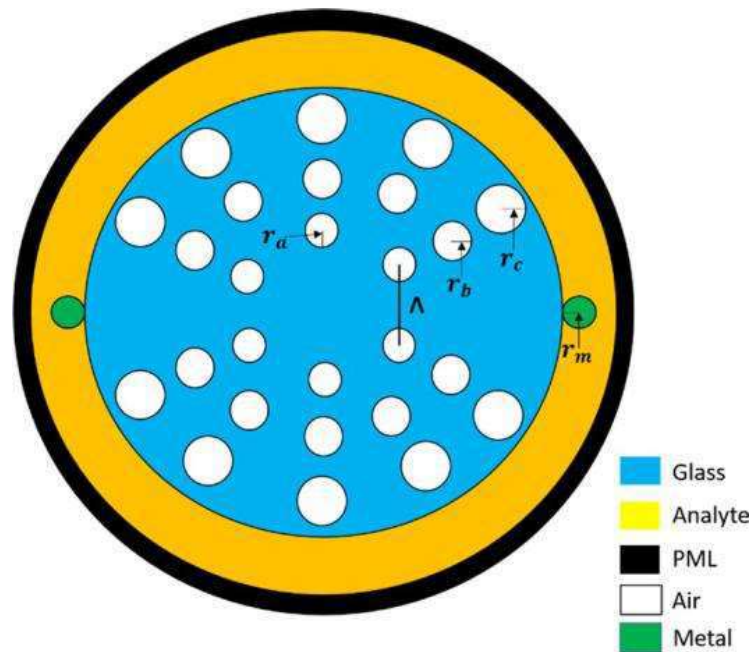


Figure 2.1 Cross section of proposed PCF sensor

Air holes of the first layer have taken of radius $r_a = 0.37 \mu\text{m}$ with pitch $\Lambda = 1.5 \mu\text{m}$. The radii of outer layer holes are $r_b = 0.50 \mu\text{m}$ and $r_c = 0.70 \mu\text{m}$, respectively. To reduce the confinement of light in the metal–dielectric interface, we choose large air holes in the outermost layer¹⁰³.

Chapter 2: Metal wires assisted PCF based refractive index sensor

The radius of the metal wire has been taken $r_m = 0.38 \mu\text{m}$. We have simulated the structure several times to optimize the values of structural parameters for higher sensitivity. The COMSOL Multiphysics simulation software has used to characterize the performances of the proposed sensor¹⁰⁴. Variations of inner and outer hole radius are taken from $r_a = 0.31 - 0.37 \mu\text{m}$, $r_b = 0.50 - 0.60 \mu\text{m}$ and $r_c = 0.70 - 0.90 \mu\text{m}$, respectively. Metal wire radius varies from $r_m = 0.38-0.46 \mu\text{m}$. The range of analyte is taken from refractive index 1.31 – 1.36. There is the presence of scattering boundary conditions and the perfect match layer (PML), which surrounds the computational domain and theoretically absorbs any wave traveling towards boundaries without reflections¹⁰⁵. The thickness of PML is taken 10% to the radius of the fiber. The material used in the background is fused silica whose refractive index is given by Sellmeier's equation¹⁰⁶

$$\mathbf{n}^2(\lambda) = \mathbf{1} + \frac{A_1\lambda^2}{\lambda^2 - B_1} + \frac{A_2\lambda^2}{\lambda^2 - B_2} + \frac{A_3\lambda^2}{\lambda^2 - B_3} \quad (2.1)$$

Here constants B_1, B_2, B_3, C_1, C_2 and C_3 are the sellmeier's constant with values 0.696163, 0.4079462, 0.8974794, 0.000467914826 μm^2 , 0.0135120631 μm^2 , 97.9340025 μm^2 , respectively. The Refractive indices of the materials of copper, silver, and gold are obtained by the Lorentz - Drude Model¹⁰⁷. The cladding region has a finite number of air holes, so there is an escape of light to external material from core known as confinement loss¹⁰⁸. We have performed the simulation to compute the mode and the effective refractive index of the proposed PCF sensor. To calculate the confinement loss, we use the imaginary part of effective refractive index. The expression for confinement loss estimation is given by eq. (1.7).

Chapter 2: Metal wires assisted PCF based refractive index sensor

where, λ represents the wavelength in μm . Hexagonal air-filling holes bounded most of the energy due to reduced core refractive index, and a small amount of energy is leaked through the cladding holes to the metal wire surface. This amount of energy prompts metal wire to yield surface plasmon resonance ¹⁰⁹.

2.3 Simulation result and discussion

Evanescent field and metal surface electrons interactions are the main factors for metals wire assisted PCF sensor mechanism ¹¹⁰. This interaction takes place at the interface of metal-dielectric. The performance of the sensor depends on the structural parameter of the PCF. Sensitivity can be increased by making the strong coupling between surface plasmon polariton (SPP) and core-guided modes. Figure 2.2 (a) shows the distribution of real and imaginary parts of the effective refractive index of copper. On increasing the wavelength, the value of the imaginary part of the effective refractive index increases and reaches a maximum value and then decreases. This is because, initially, the coupling between SPP mode and Core mode increases with an increase in wavelength, then reaches its maximum value. After that, the coupling gets weakened, and hence loss decreases. Electric field distribution for the peak point is depicted in figure 2.2 (b). At this peak point, we observe strong coupling between fundamental and SPP modes. The peak points for copper, gold, and silver are at wavelength 778 nm, 850 nm, and 756 nm with a loss of 39.00 dB/cm, 64.95 dB/cm, and 52.79 dB/cm, respectively. The detection range of the refractive index for copper metal is from 1.31 to 1.36, while for gold and silver metals; it is from 1.31 to 1.35.

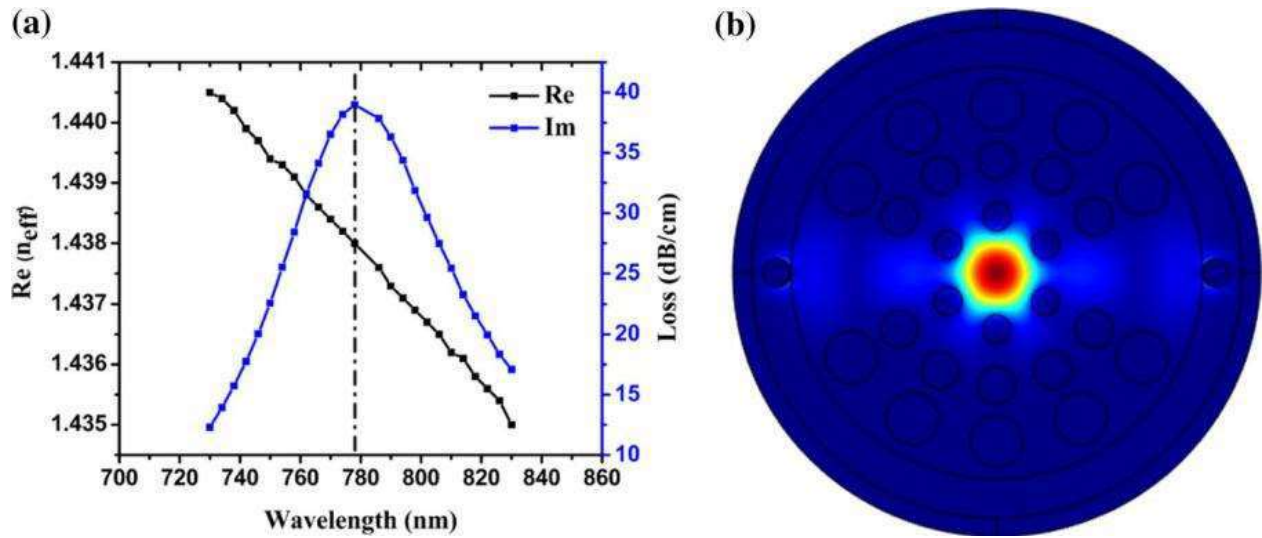


Figure 2.2 (a) Real and Imaginary part of effective refractive index for Cu (b) SPR appearance of Cu for $r_a = 0.37 \mu\text{m}$, $r_b = 0.50 \mu\text{m}$, $r_c = 0.70 \mu\text{m}$, $r_m = 0.38 \mu\text{m}$, and $n_a = 1.34$.

The proposed sensor characteristics are affected by structural parameters, such as air hole radius and metal wire radius. Confinement losses for copper metal gently increase from peak value 755 to 778 nm with a peak shift of 23 nm when the radius of inner holes varies from 0.31 to 0.37 μm . This behavior is shown in figure 2.3 (a). Similarly, the confinement losses for gold and silver are illustrated in figure 2.3 (b) and (c). For gold, peak shifts from 820 to 850 nm with a change of 30 nm, while for silver peak shift is observed from 731 to 756 nm with a change of 25 nm. This result is due to the change of radius r_a of metal wires. As the radius r_a increases, the air filling fraction (AFF) of the core is reduced which results the maximum amount of energy possibly to escape from the core to the cladding and hence it increases the loss.

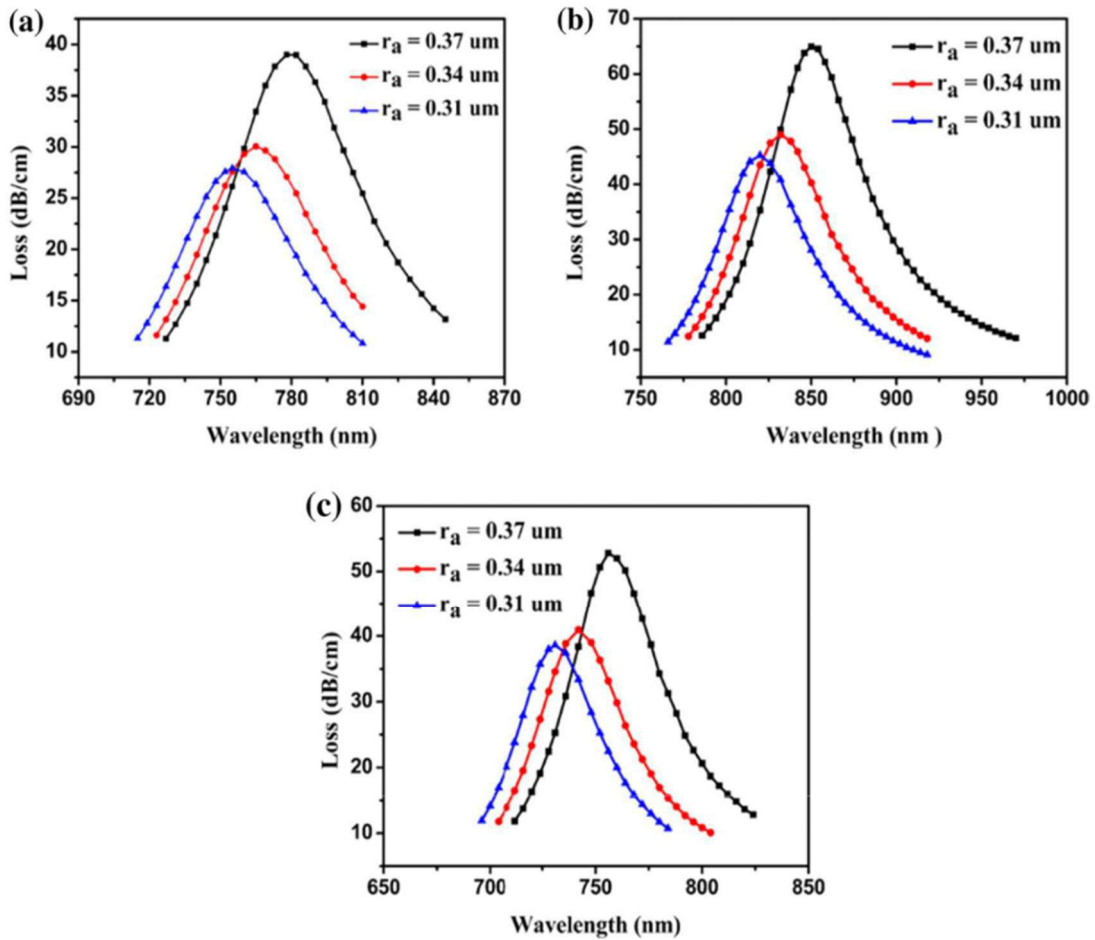


Figure 2.3 Loss spectra for different radii of inner air holes in the structures for (a) Copper (b) Gold (c) Silver with $r_b = 0.50 \mu\text{m}$, $r_c = 0.70 \mu\text{m}$, $r_m = 0.38 \mu\text{m}$ and $n_a = 1.34$.

A higher radius of air holes in the outer area is required because having large air holes in cladding reduces its refractive index. Figure 2.4 shows the effect of the second layer of air holes of radius r_b on the confinement loss for all considered metals. Increasing the radius from 0.50 to $0.60 \mu\text{m}$, sensor intensity reduces from 39 to 14.24 dB/cm for copper, from 64.95 to 23.78 dB/cm for gold, and from 52.79 to 19.02 dB/cm for silver because of reduction in effective index, respectively.

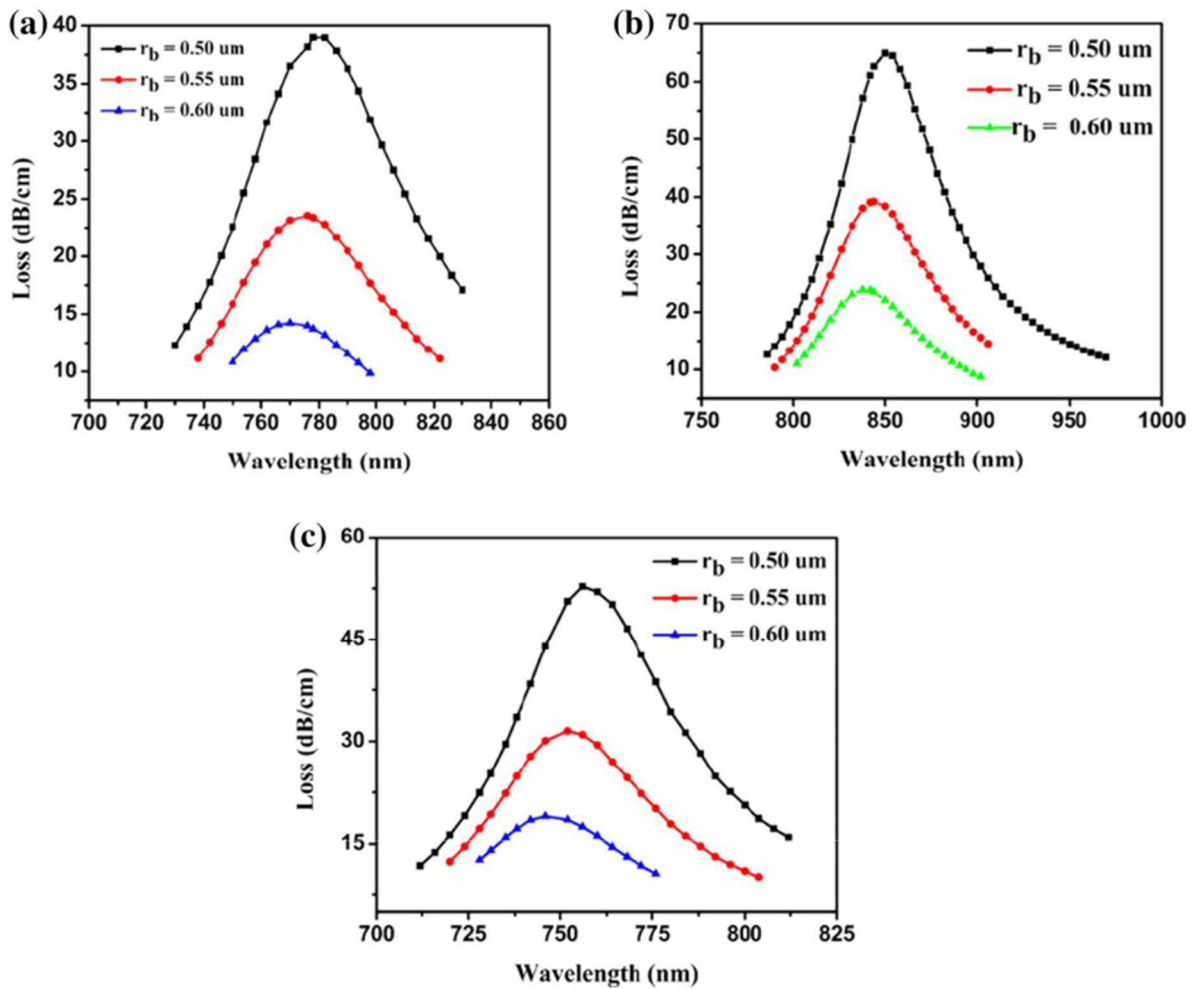


Figure 2.4 Loss spectra for different radii of inner air holes in the structures for (a) Copper (b) Gold (c) Silver with $r_a = 0.37 \mu\text{m}$, $r_c = 0.70 \mu\text{m}$, $r_m = 0.38 \mu\text{m}$ and $n_a = 1.34$.

The effect of the third layer air hole radius on the confinement loss is shown in figure 2.5 (a), (b) and (c). Changing of the radius r_c from 0.70 to 0.90 μm , loss reduces 39.00 dB/cm – 34.37 dB/cm for copper, 64.95 dB/cm – 54.75 dB/cm for gold, and 52.79 dB/cm – 46.73 dB/cm for silver respectively. So it is clear that the reduction of confinement loss achieves with an increase of the radius.

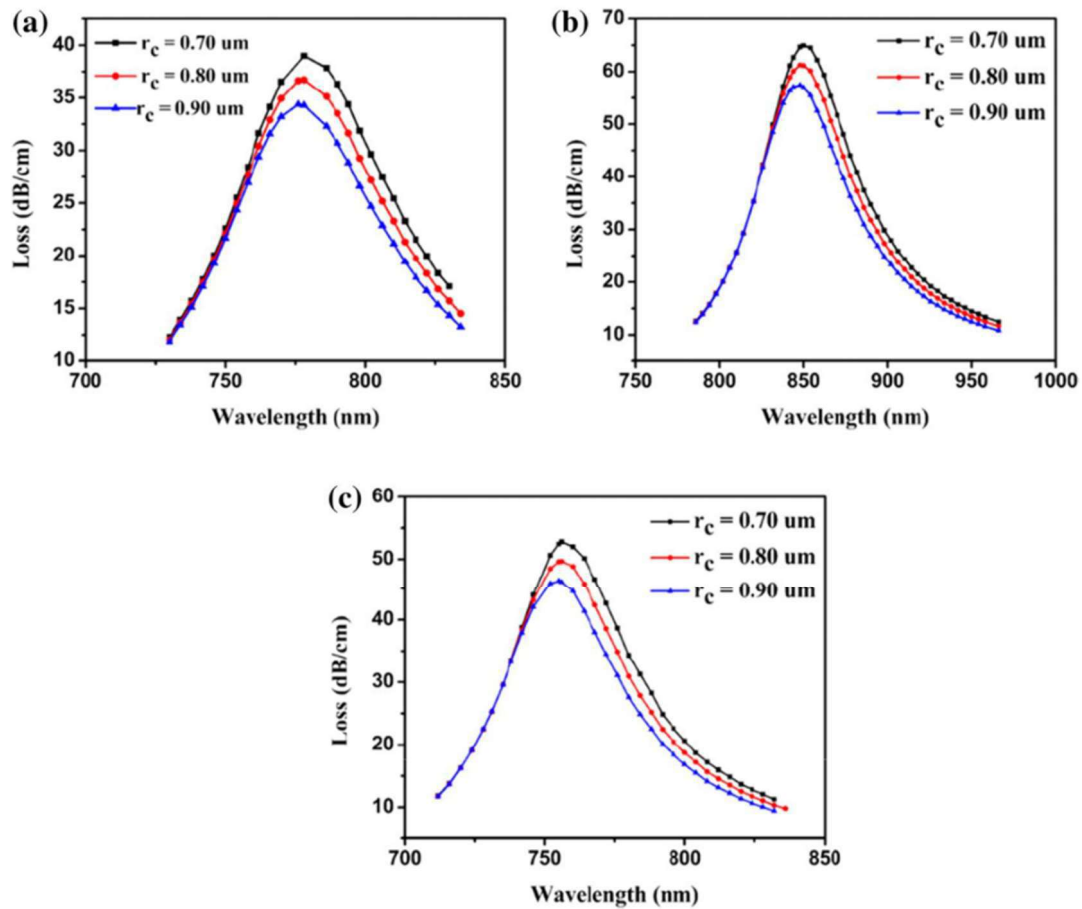


Figure 2.5 Loss spectra for different radii of inner air holes in the structures for (a) Copper (b) Gold (c) Silver with $r_a = 0.37 \mu\text{m}$, $r_b = 0.50 \mu\text{m}$, $r_m = 0.38 \mu\text{m}$ and $n_a = 1.34$.

In order to find the effect of metal wire radius on sensing performance, the radius of metal wire has increased from 0.38 to $0.46 \mu\text{m}$. It is clear from figure 2.6 that sensor's loss peak intensity reduces with increasing the radius of the metal ring. Higher damping loss occurs due to increase of diameter of metal wire. This is because on increasing the diameter of metal wire it becomes difficult for evanescent wave to penetrate on sensing layer which results weak SPR coupling^{111 112}. Intensities reduce about 3 dB/cm , 8 dB/cm , and 5 dB/cm for the structures with Cu, Au, and Ag wires, respectively.

Chapter 2: Metal wires assisted PCF based refractive index sensor

The sensitivity is an important parameter to demonstrate the performance of the sensor. A low-cost sensor with better sensitivity is important for sensing applications. We have taken metals Cu, Au, and Ag to find the best of them in sensitivity and compatibility with the proposed sensor structure. The sensor response has investigated for different analytes of RI 1.31–1.36. The n_{eff} of SPP mode depends on the refractive index of a surrounding medium, so when there is a slight change in RI of the medium, that leads to the change in n_{eff} of SPP and resonance wavelength shifts. The sensitivity of an optical fiber sensor depends on the resonance wavelength peak shift and RI difference.

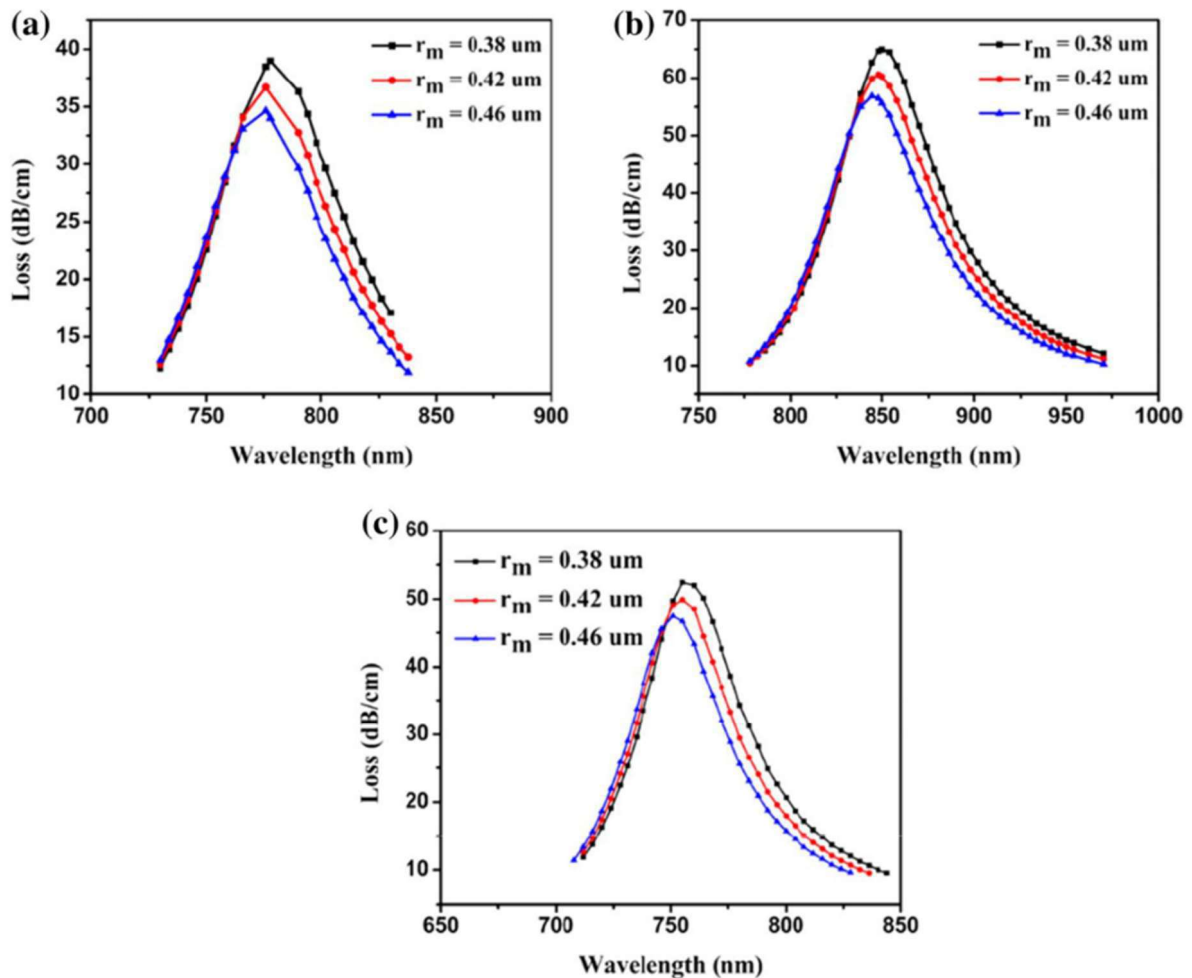


Figure 2.6 Loss spectra for different radii of inner air holes in the structures for (a) Copper (b) Gold (c) Silver with $r_a = 0.37 \mu\text{m}$, $r_b = 0.50 \mu\text{m}$, $r_c = 0.70 \mu\text{m}$ and $n_a = 1.34$.

Chapter 2: Metal wires assisted PCF based refractive index sensor

We have used a wavelength interrogation method to calculate the wavelength spectral sensitivity S given by the equation ¹¹³

$$S_{\lambda} = \frac{\Delta\lambda_{peak}}{\Delta n_a} \text{ (nm/RIU)} \quad (2.2)$$

Where $\Delta\lambda_{peak}$ peak represents the peak shift of resonance wavelength and Δn_a is a change in refractive index of analyte.

Figure 2.7 shows the confinement loss vs. wavelength graph for different metals. We find that the peak shift for copper wire assisted sensor is 73 dB/cm for the analyte of RI from 1.35 to 1.36. This result provides the maximum sensitivity of 7300 dB/cm and average sensitivity of 4320 nm/RIU for the range of RI 1.31 – 1.36. However, the peak shifts are 62 nm and 61 nm for gold and silver for RI 1.34 – 1.35, so the maximum sensitivities are 6200 and 6100 nm/RIU, respectively. Average sensitivities for range 1.31 – 1.35 are 4275 nm/RIU and 3950 nm/RIU for gold and silver, respectively. Due to a maximum peak shift in wavelength for copper metal, we have chosen this metal for further analysis.

Amplitude sensitivity method is also applied to calculate the sensor sensitivity, and its formula is given by ⁹⁷

$$S_A \text{ (RIU}^{-1}\text{)} = - \frac{1}{\alpha(\lambda, n_a)} \times \frac{\partial\alpha(\lambda, n_a)}{\partial n_a} \quad (2.3)$$

Where, $\alpha(\lambda, n_a)$ represents the confinement loss for the analyte of RI (n_a) and $\partial\alpha(\lambda, n_a)$ is called confinement loss difference between two adjacent RI of analytes for the same wavelength.

Chapter 2: Metal wires assisted PCF based refractive index sensor

Figure 2.8 shows copper metal gives maximum amplitude sensitivity 597 RIU^{-1} at a particular wavelength of 908 nm for RI 1.35 while Au and Ag provide maximum amplitude sensitivity 422 RIU^{-1} and 560 RIU^{-1} at wavelength 922 nm and 824 nm for analyte RI 1.34, respectively. So it is clear that Cu provides maximum amplitude sensitivity among the considered metals, and Cu is showing maximum amplitude sensitivity for analyte RI more than 1.34 while Au and Ag are showing maximum amplitude sensitivity for analyte RI 1.34.

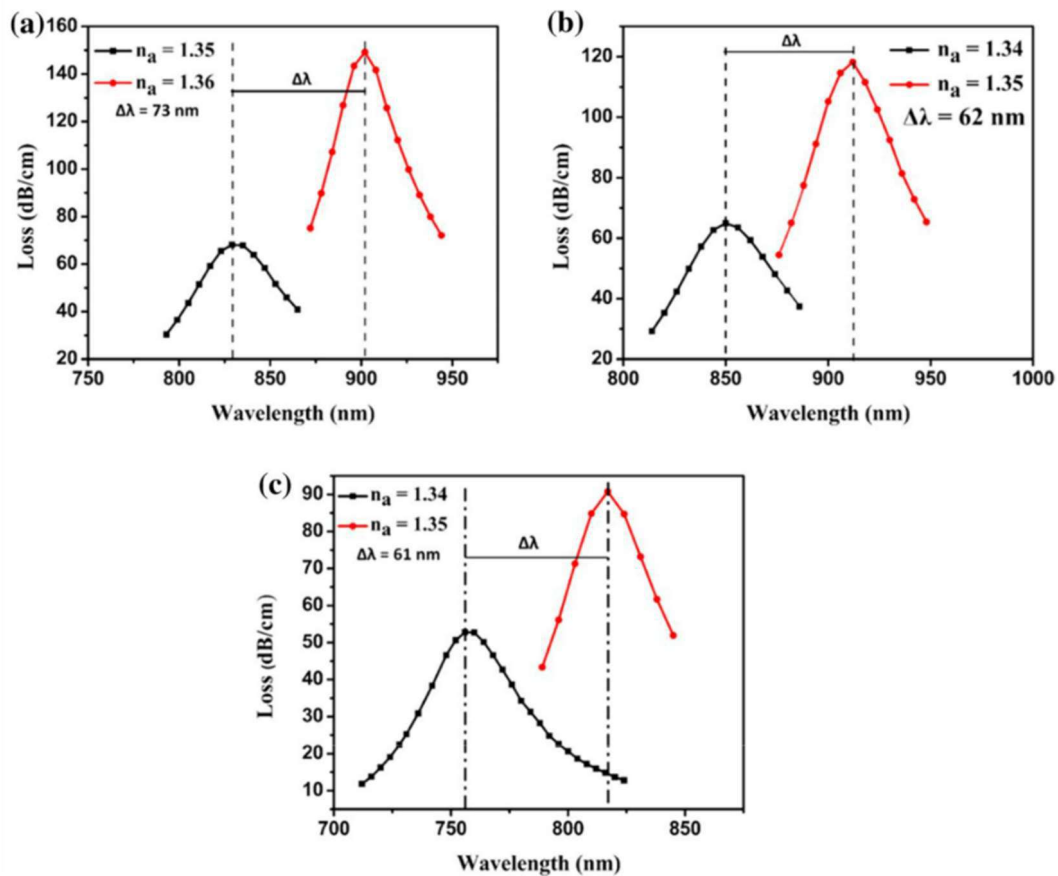


Figure 2.7 Peak shift for the structure with metal wires of (a) Cu (b) Au (c) Ag for $r_a = 0.37 \mu\text{m}$, $r_b = 0.50 \mu\text{m}$, $r_c = 0.70 \mu\text{m}$, $r_m = 0.37 \mu\text{m}$, and $n_a = 1.34$.

Chapter 2: Metal wires assisted PCF based refractive index sensor

Wavelength Resolution is also an essential parameter of sensor which is calculated by the formula

111

$$R (RIU) = \Delta n_a \times \frac{\Delta \lambda_{min}}{\Delta \lambda_{peak}} \quad (2.4)$$

Where, $\Delta \lambda_{min} = 0.1$ nm represents the smallest spectral resolution. For Cu, the maximum resolution is 1.37×10^{-5} RIU, while for Au and Ag, it reaches up to 1.61×10^{-5} RIU and 1.63×10^{-5} RIU, respectively

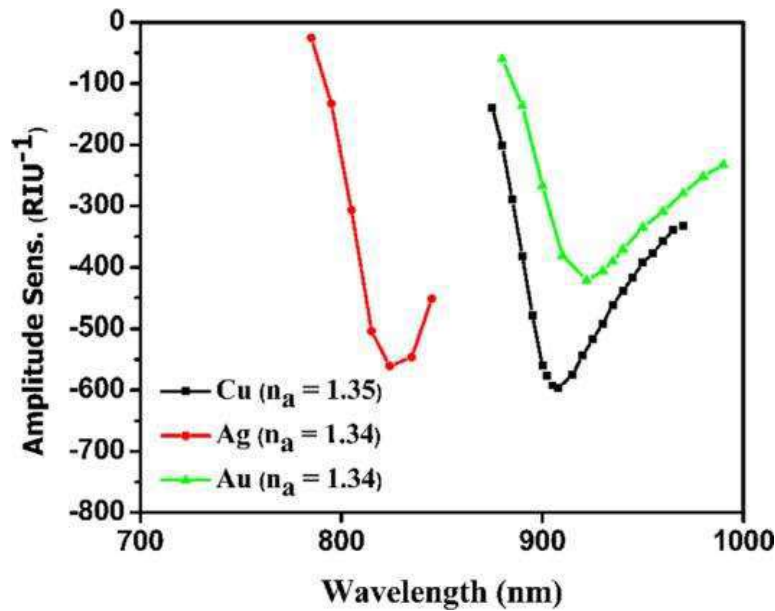


Figure 2.8 Comparison of maximum amplitude Sensitivity (RIU⁻¹) for Cu (Black), Ag (Red), and Au (Green)

We have tabulated the results for the proposed sensor structure in tables 2.1, table 2.2, and table 2.3 for copper, gold, and silver metals, respectively. It is clear from tables that the result for Cu is better than other considered metals.

Chapter 2: Metal wires assisted PCF based refractive index sensor

Compare to the previously reported sensors^{114 115 116 117} using gold as a plasmonic material in their proposed structure for sensing purpose, we have demonstrated copper as a plasmonic material for our proposed structure with improved sensitivity and resolution, and the copper is providing better results in terms of maximum wavelength sensitivity (S), maximum amplitude sensitivity compare to the gold and silver. Sensor resolution with less confinement loss for our proposed structure as well as it is cost effective than that of gold and silver metal. A wide comparison of the proposed sensor with other available sensors in terms of refractive index range, confinement loss, maximum sensitivity, and amplitude sensitivity is revealed in table 2.4. We observe that our proposed copper metal wire based structure has improved results as compared to others. Figure 2.9 shows the polynomial fitting of the variation of analyte RI with wavelength. To see how close the data are to the fitted regression line, we have represented a statistical measurement in terms of R^2 . In the figure, the values of R^2 are 0.99670 for Cu, 0.99814, and 0.99915 for Au and Ag, respectively. The value of R^2 for Cu is approximately equal to gold and silver.

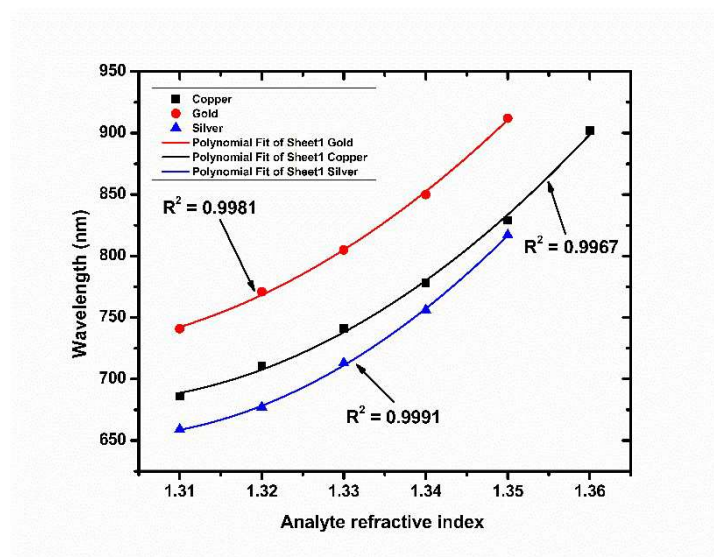


Figure 2.9 Variation between resonant wavelength and RI of analyte.

Chapter 2: Metal wires assisted PCF based refractive index sensor

Table 2.1 Performance of the proposed PCF sensor with copper metal wire

Analyte (RI)	Peak loss (dB/cm)	Resonance wavelength (nm)	Peak shift wavelength (nm)	Sensitivity (nm/RIU)	Wavelength Resolution (RIU)
1.31	11.65	686	25	2500	4.00×10^{-5}
1.32	16.55	711	30	3000	3.33×10^{-5}
1.33	24.61	741	37	3700	2.70×10^{-5}
1.34	39.00	778	51	5100	1.96×10^{-5}
1.35	68.14	829	73	7300	1.36×10^{-5}
1.36	149.16	902	-	-	-

Table 2.2 Performance of the proposed PCF sensor with gold metal wire

Analyte (RI)	Peak loss (dB/cm)	Resonance wavelength (nm)	Peak shift wavelength (nm)	Sensitivity (nm/RIU)	Wavelength Resolution (RIU)
1.31	19.41	741	30	3000	3.33×10^{-5}
1.32	27.49	771	34	3400	2.94×10^{-5}
1.33	40.95	805	45	4500	2.22×10^{-5}
1.34	64.95	850	62	6200	1.61×10^{-5}
1.35	118.21	912	-	-	-
1.36	-	-	-	-	-

Chapter 2: Metal wires assisted PCF based refractive index sensor

Table 2.3 Performance of the proposed PCF sensor with silver metal wire

Analyte (RI)	Peak loss (dB/cm)	Resonance wavelength (nm)	Peak shift wavelength (nm)	Sensitivity (nm/RIU)	Wavelength Resolution (RIU)
1.31	14.85	659	18	1800	5.55×10^{-5}
1.32	24.90	677	36	3600	2.77×10^{-5}
1.33	34.99	713	43	4300	2.33×10^{-5}
1.34	52.79	756	61	6100	1.63×10^{-5}
1.35	90.77	817	-	-	-
1.36	-	-	-	-	-

Table 2.4 Comparison of our proposed sensor structure with other available sensors solely based on simulation

References	PCF Type	Analyte range	Wavelength Resolution (RIU)	Sensitivity (nm/RIU)	Amplitude Sensitivity (RIU ⁻¹)
⁹⁵	Gold coated PCF	1.33 – 1.36	3.75×10^{-5}	2200	266
¹¹⁷	Graphene - Based PCF	1.33 – 1.35	3.97×10^{-5}	2520	44
¹¹⁵	Gold Nano shell PCF	1.33 – 1.38	2.45×10^{-5}	4114	-
¹¹⁸	Dual channel PCF sensor	1.30 – 1.40	-	3750	40
⁹⁷	Open channel based PCF	1.33 – 1.39	2.0×10^{-5}	5000	396
Our work	PCF with Cu metal wire	1.31 – 1.36	1.36×10^{-5}	7300	597

Chapter 2: Metal wires assisted PCF based refractive index sensor

2.4 Conclusion

We have modeled and simulated metals wire assisted solid-core PCF sensors using different metal wires to produce the SPR effect for RI sensing applications. We have obtained maximum sensitivity 7300 nm/RIU with maximum amplitude sensitivity 597 RIU⁻¹ and wave-length resolution 1.36×10^{-5} RIU for RI 1.35 for copper metal. However, the maximum sensitivity is 6200 nm/RIU, maximum amplitude sensitivity 422 RIU⁻¹, and its wavelength resolution 1.61×10^{-5} RIU for RI 1.34 with Au while maximum sensitivity 6100 nm/RIU, maximum amplitude sensitivity 560 RIU⁻¹ and wavelength resolution 1.63×10^{-5} RIU for RI 1.34 with Ag. Thus, we observe that copper is providing better results in terms of sensitivity and resolution among considered metals. Overall, the proposed sensor is a simple structure that provides less confinement loss and higher sensitivity for copper metal which is cheaper than gold and silver. According to our results, the SPR based PCF sensor has a wide application and great potential for a wide range of refractive index analyte detection.

